Respiratory Research

RESEARCH

Open Access

MiR-1307-5p enhances fibroblast transdifferentiation to exacerbate chronic obstructive pulmonary disease through regulating FBXL16/HIF1α axis

Li-peng Yao[1,2,5†], Zheng-kai Wang[1,5†], Xin-qing Jiang[3†], Beier Jiang[4†], Si-jia Chen[4], Zhi-dan Hua[5], Dan-dan Gao[1], Quan Zheng[4], Sheng-mei Zhu[4], Mao-xiang Qian[6], Feng Zhang[4*], Li-feng Xu[4*], Cheng-shui Chen[1,5,7*] and Fang Lu[5*]

Abstract

Chronic obstructive pulmonary disease (COPD) is an irreversible and progressive chronic inflammatory lung disease which affects millions of people worldwide. Activated fibroblasts are observed to accumulate in lung of COPD patients and promote COPD progression through aberrant extracellular matrix (ECM) deposition. In this study, we identified that miR-1307-5p expression was significantly increased in lung fibroblasts derived from COPD patients. Mechanistically, we found that upregulation of miR-1307-5p promoted TGF-β induced lung fibroblast activation and transdifferentiation. We also identified FBXL16 as a direct target for miR-1307-5p mediated myofibroblast activation in COPD. Knockdown of FBXL16 by siRNA prominently increased the expression of myofibroblast markers in MRC-5 fibroblasts after TGF-β administration. Ectopic expression of FBXL16 in MRC-5 counteracted miR-1307-5p agomir-induced fibroblast transdifferentiation. Furthermore, We found that miR-1307-5p promoted pulmonary fibroblast transdifferentiation through FBXL16 regulated HIF1α degradation. In general, our findings indicate that miR-1307-5p is important for COPD pathogenesis, and may serve as a potential target for COPD treatment.

Keywords COPD, miR-1307-5p, FBXL16, HIF1α, Lung fibroblast, Transdifferentiation

†Li-peng Yao, Zheng-kai Wang, Xin-qing Jiang, Beier Jiang these authors contributed equally.

*Correspondence:
Feng Zhang
fengzhang@wmu.edu.cn
Li-feng Xu
qz1109@wmu.edu.cn
Cheng-shui Chen
wzchencs@163.com
Fang Lu
lufang@wmu.edu.cn
[1]Wenzhou Medical University, Wenzhou 325035, China
[2]Ningbo College of Health Sciences, Ningbo 315000, China
[3]Zhejiang Chinese Medical University, the 2nd Clinical Medical College, Hangzhou 310053, China
[4]Joint Innovation Center for Engineering in Medicine, Quzhou Affiliated Hospital of Wenzhou Medical University, Quzhou 324000, China
[5]Department of Respiratory and Critical Care, the Quzhou Affiliated Hospital of Wenzhou Medical University, Quzhou 324000, China
[6]Institute of Pediatrics and Department of Hematology and Oncology, Children's Hospital of Fudan University, Shanghai 200032, China
[7]The Key Laboratory of Interventional Pulmonology of Zhejiang Province, Department of Pulmonary and Critical Care Medicine, Centre of Precision Medicine, The First Affiliated Hospital of Wenzhou Medical University, Wenzhou 325015, China

Introduction

COPD is an irreversible and progressive chronic inflammatory lung disease which affects millions of people worldwide, particularly impacting the elderly population due to the natural decline in lung function that occurs with age. The disease is characterized by chronic bronchitis and emphysema [1, 2]. In addition to smoking, which is the most important risk factor for COPD, with the smoking index is positively correlated with the severity of COPD disease, air pollution also plays a significant role in the development of COPD. Long-term exposure to polluted air can lead to a persistent inflammatory response in the lungs, contributing to the pathogenesis of COPD. Smoking induced airway epithelium disruption and deregulated remodeling are considered to be pivotal to COPD pathogenesis. An imbalance between ECM deposition and degradation is one of the major mechanisms of COPD airway remodeling [3]. The combination of age-related lung function decline and environmental pollutants creates a synergistic effect that can exacerbate the condition.

ECM plays a critical role in maintaining the normal structure and function of the lungs. It is an important mediator to protect against lung tissue damage. However, excessive ECM synthesis and accumulation in pathological states can have a direct impact on airway structure, leading to abnormal structural construction of the airway wall, destruction of lung parenchyma, and interstitial hyperplasia, exacerbating airway fibrosis and obstructing airway airflow [4]. The main sources of airway ECM components are pulmonary fibroblasts and myofibroblasts. The transdifferentiation of pulmonary fibroblast is crucial in the increase of ECM accumulation and airway remodeling in COPD [5].

Fibroblasts are lung structural cells whose major function is to maintain the lung and repair damage [6]. In response to injury, fibroblasts differentiate and become activated as myofibroblasts with the help of pro-fibrotic mediators such as TGF-β, and express high level of alpha smooth muscle actin (α-SMA). These fibroblasts release proteases to cleave the damaged ECM to allow access for other cells and new ECM deposition. Myofibroblasts also release cytokines and chemokines to signal and recruit immune cells and deposit ECM [7]. Additionally, activated fibroblasts possess contractile characteristics that aid in the process of wound closure [8].

Whilst physiologically, fibroblasts play a key role in lung repair, if they become dysfunctional, they can promote aberrant tissue remodeling. In COPD patients, the airway epithelium produces more TGF-β, resulting in a pro-fibrotic milieu around the airways that promotes fibroblast activation [9]. In COPD lung tissue, there is an accumulation of activated fibroblasts and elevated α-SMA expression [10]. These fibroblasts also have altered expression of pro-fibrotic markers, with evidence for enhanced TGF-β and ECM gene expression, such as COL1A1 and COL3A1, as compared to smoker/non-smoker control fibroblasts [11]. This suggests fibroblasts are responsible for the deregulated ECM deposition and therefore are implicated in the development of COPD.

MicroRNAs, also known as miRNAs, are a type of non-protein-coding regulatory RNA that is around 22 nucleotides long [12]. MiRNAs pair with mRNAs according to the principle of base complementarity, and inhibit the translation of target mRNAs or promote the degradation of mRNAs, thus reducing the protein products of targeted mRNAs [13]. Numerous studies have found that miRNAs are closely linked to the development of COPD [14]. MiR-1307-5p is functionally a less well-studied miRNA. It was reported to target TRAF3 and activate the MAPK/NF-κB pathway to promotes lung adenocarcinoma proliferation [15].

In our previous COPD population-based cohort study, we found that miR-1307-5p was increased in the blood samples from COPD patients. In this study, we identified that the majority of up-regulated miR-1307-5p expression was in lung fibroblasts. Mechanistically, we found that upregulation of miR-1307-5p promoted lung myofibroblast activation. We also identified FBXL16 as a direct target for miR-1307-5p mediated myofibroblast activation in COPD progression. Furthermore, we determined that HIF1α mediates FBXL16 regulated fibroblast activation. Our findings indicate that miR-1307-5p is important for COPD pathogenesis, and may serve as a potential target for COPD treatment.

Materials and methods

Induction of experimental COPD

Eight to ten-week-old male C57BL/6 mice were procured from Vital River Laboratory Animal Technology (Beijing, China) and housed under sterile conditions with a 12-hour light/dark cycle, allowing for a one-week acclimatization period. To induce experimental COPD, mice were subjected to chronic exposure to cigarette smoke from Chinese Lion cigarettes or normal air through nasal inhalation for 75 min, twice daily, five days a week for 16 weeks. For miRNA agomir intervention, mice were intranasally administered with MiR-1307-5p specific or scrambled antagomir once a week (2.5 mg/kg) under isoflurane anesthesia. For FBXL16 overexpression in lung tissues, mice were intranasally administered with control or FBXL16 expressing AAV6 twice, at the 4th and 8th weeks, under isoflurane anesthesia. All animal experiments were conducted following protocols approved by the Laboratory Animal Management and Ethics Committee of Hangzhou Medical College in Zhejiang Province (license number of animal use permit: SYXK 2023-0011,

license number of approval of animal ethical and welfare: ZJCLA-IACUC-202387).

Pulmonary function assessment

Pulmonary function tests were conducted using a forced pulmonary maneuver system (Shanghai Yuyan Instrument Co., Ltd.), following the manufacturer's instructions and established protocols [16]. Mice were anesthetized with ketamine (100 mg/kg) and xylazine (10 mg/kg), followed by tracheal cannulation. Each maneuver was performed three times, and the average results were calculated.

Human subjects

Normal and COPD lung tissue specimens were obtained from patients who underwent lobectomy or pneumonectomy for lung cancer in the Quzhou Affiliated Hospital of Wenzhou Medical University. COPD was diagnosed based on a combination of medical history and physical examination including pulmonary function test using spirometry. Informed written consent was obtained from all participants. All studies have been approved by the Institutional Review Board at the Quzhou Affiliated Hospital of Wenzhou Medical University (permission No.2021-03-005). The basic medical information of the volunteers was listed in Table 1. Each patient signed an informed consent form for sample collection.

Cell culture

Human lung fibroblast MRC-5 and HEK293T cells was purchased from Cell Bank of the Chinese Academy of Sciences (Shanghai, China) and was cultured in DMEM containing 10% FBS and antibiotics in 5% CO_2 at 37℃ in a humidified atmosphere.

Isolation of primary lung fibroblasts and epithelial cells

Primary human lung fibroblasts and lung epithelial cells were isolated as described previously [17]. Lung tissues were cut into small pieces and incubated with digestion buffer (0.1% collagenase, 0.05% trypsin, and 100 mg/mL DNase in Hanks' balanced salt solution) for 1 h at 37℃. The digested tissue suspensions were filtered through a 40 μm cell strainer, centrifuged at 500×g for 5 min and pellets were collected. After the lysis of red blood cells, the cells were resuspended and incubated for 1 h with biotin-conjugated anti-CD16/32, anti-CD45, and anti-CD31 antibodies. The cells were then rinsed, resuspended, and incubated for 30 min with streptavidin magnetic beads. Tubes containing the incubated cells were then applied to a magnet to deplete endothelial cells, lymphocytes, monocytes/macrophages, natural killer (NK) cells, neutrophils, and other haematopoietic cells. Supernatants were collected and plated into tissue culture plates. After 1 h incubation at 37 ℃, the suspended lung epithelial cells were harvested for experiments. The adherent lung fibroblasts were grown in MEM media supplemented with 10% FBS. Fibroblasts at passage 3–5 were used for experiments.

Plasmids, transfection and lentiviral infection

miR-1307-5p agomir (HY-R00240A) and antagomir (HY-RI00240A) were purchased from MedChemExpress LLC (Shanghai, China). Compared with common mimics/inhibitors, miRNA agomir/antagomir has higher stability and inhibitory effect in mammalian cells, and is more likely to pass through cell membranes to be enriched in target cells. Cells were transfected in 6-well plates using RNAiMAX transfection reagent (Life Technologies, Thermo Fisher Scientific) and OptiMEM media according to manufacturer's instruction.

For FBXL16 expression in MRC-5 cells, the cDNA ORF clone was purchased from Sino Biological (Cat# HG24168-UT). Then the FBXL16 cDNA ORF fragment was subcloned into pCDH-CMV-puro lentiviral expression vector. The method for lentivirus production and transduction was introduced previously [18]. FBXL16 miRNA 3'-UTR clone (#MiUTR1R-01841) in pMirTarget 3'-UTR Assay Vector was ordered from Creative Biogene (NY, USA). Mutated 3'-UTR of FBXL16 was generated using the Hieff Mut™ Site-Directed Mutagenesis Kit (YEASEN, Shanghai, China). Lipofectamine 3000 reagents were performed for transfection according to

Table 1 Patient characteristics for mir-1307-5p analysis

	Healthy control	COPD	*p* value
Number	6	6	
Age (years)	56.3 (8.2)	63.6 (8.4)	n.s.
BMI	25.2 (4.1)	26.1 (3.8)	n.s.
Sex (M/F)	3/3	3/3	
Smoking history (pack-years)	0	42.1 (22.3)	<0.01
FEV1/FVC, mean (SD)	79.6 (8.13)	62.8 (10.92)	<0.01
FEV1, mean (SD)	90.3 (7.51)	71.5 (11.57)	<0.01
GOLD (n) 0/I/II/III/IV	6/0/0/0/0	0/0/2/3/1	

Notes: GOLD, Global Initiative for Chronic Obstructive Lung Disease; Forced Vital Capacity, forced vital capacity; FEV1, forced expiratory volume in 1 s. Data are expressed as mean (SD)

the manufacturer's instruction (Invitrogen). HA-Clover-HIF-1α wild-type (#163365) and HA-Clover-HIF-1α S31D (#163370) were ordered from Addgene.

Real-time PCR

The extraction of total RNA was performed utilizing Trizol reagent in conjunction with the conventional liquid phase method incorporating chloroform. The RNA sample underwent reverse transcription to generate complementary DNA (cDNA) utilizing the RT-Mix kit (Takara, RR036A) with either random primer or gene specific RT primer. The real time PCR experiment was conducted using the SGExcel FastSYBR Master premix (Sangon Biotech, B532955-0005) following standard reaction conditions. The primers employed in this experiment are documented in Table 2. The relative expression level of the target gene or miRNA was determined utilising the $2^{-\Delta\Delta Ct}$ methodology, with β-actin or U6 serving as the internal reference gene.

Western blotting

Cells were washed with 1× PBS and lysed in 1× SDS buffer containing protease inhibitors. The lysate was collected, boiled at 100 °C for 10 min, and centrifuged to remove cell debris. Equal amounts of protein were separated by SDS-PAGE and transferred onto a PVDF membrane. The membrane was blocked with 0.1% casein at room temperature for 60 min and then incubated overnight at 4 °C with the appropriate primary antibodies. Subsequently, the membrane was incubated with an HRP-conjugated secondary antibody at room temperature for about 60 min. Finally, the protein bands were detected using an ECL protein blotting substrate. The antibodies used for western blotting were listed in Table 3. The intensity of bands was quantified using the Image J software.

ELISA

The levels of proteins in lung tissue homogenates were quantified using ELISA kits listed in Table 3, following the manufacturer's instructions. Lung tissue homogenates were prepared by rapidly freezing and homogenizing on ice in RIPA buffer (Beyotime, #R0010) with phenylmethylsulfonyl fluoride (PMSF). The homogenates were sonicated three times for 5 s each, centrifuged at 500× g for 10 min at 4℃, and the central layer was collected. Total protein concentrations were determined using a BCA Protein Assay Kit (Thermo Fisher Scientific Pierce). Lung tissue homogenates were then diluted with RIPA buffer to a final protein concentration of 500 mg/mL. For consistency, the obtained values were normalized to the total protein content.

Table 2 Sequence of primers used for miRNA agomir, antagomir and qRT-PCR

Primer name	Sequences (5′→3′)	Species	Application
miR-1307-5p agomir	UCGACCGGACCUCGACCGGCU	human	overexpression
miR-1307-5p antagomir	AGCCGGUCGAGGUCCGGUC	human	inhibition
miR-1307-5p RT	GTCGTATCCAGTGCGTGTCGTGGAGTCGGCAATTGCACTGGATACGACAGCCGG	human	reverse-transcription
U6 RT	AACGCTTCACGAATTTGCGT	human	reverse-transcription
miR-1307-5p Fwd	TCGACCGGACCTCGA	human	real-time PCR
miR-1307-5p Rev	CAGTGCGTGTCGTGGA	human	real-time PCR
U6 Fwd	CTCGCTTCGGCAGCACA	human	real-time PCR
U6 Rev	AACGCTTCACGAATTTGCGT	human	real-time PCR
α-SMA Fwd	GTGTTGCCCCTGAAGAGCAT	human	real-time PCR
α-SMA Rev	GCTGGGACATTGAAAGTCTCA	human	real-time PCR
Calponin1 Fwd	CTGTCAGCCGAGGTTAAGAAC	human	real-time PCR
Calponin1 Rev	GAGGCCGTCCATGAAGTTGTT	human	real-time PCR
Fibronectin Fwd	AGGAAGCCGAGGTTTTAACTG	human	real-time PCR
Fibronectin Rev	AGGACGCTCATAAGTGTCACC	human	real-time PCR
Collagen I Fwd	GTGCGATGACGTGATCTGTGA	human	real-time PCR
Collagen I Rev	CGGTGGTTTCTTGGTCGGT	human	real-time PCR
FBXL16 Fwd	GTGCTCGACAGGTGTGTACG	human	real-time PCR
FBXL16 Rev	GCACCATCGCAGGTAGAGG	human	real-time PCR
Cxcl1 Fwd	CTGGGATTCACCTCAAGAACATC	mouse	real-time PCR
Cxcl1 Rev	CAGGGTCAAGGCAAGCCTC	mouse	real-time PCR
TNF-α Fwd	CCCTCACACTCAGATCATCTTCT	mouse	real-time PCR
TNF-α Rev	GCTACGACGTGGGCTACAG	mouse	real-time PCR
β-actin Fwd	AGAGCTACGAGCTGCCTGAC	human	real-time PCR
β-actin Rev	AGCACTGTGTTGGCGTACAG	human	real-time PCR
β-actin Fwd	AGAGCTACGAGCTGCCTGAC	mouse	real-time PCR
β-actin Rev	AGCACTGTGTTGGCGTACAG	mouse	real-time PCR

Table 3 The reagents and antibodies used in this study

Category	Product	Source	Identifier
Antibody	anti-α-SMA	Proteintech	14395-1-AP
Antibody	anti-Calponin1	Abcam	ab46794
Antibody	anti-Fibronectin	Proteintech	15613-1-AP
Antibody	anti-Collagen I	Abcam	ab138492
Antibody	anti-HIF1α	Cell Signaling	3716
Antibody	anti-FBXL16	Bioss	bs-8474R
Antibody	anti-HA	Invitrogen	26,183
Antibody	anti-β-actin	Diagbio	db13986
Antibody	anti-α-tubulin	Abcam	ab7291
Elisa kit	TNF-α (mouse)	Cusabio	CSB-E04741m
Elisa kit	CXCL1 (mouse)	Cusabio	CSB-E17286m
Elisa kit	TGF-β (mouse)	Cusabio	CSB-E09785m
Elisa kit	TGF-β (human)	Cusabio	CSB-E09783h
Elisa kit	IL-6 (mouse)	Cusabio	CSB-E04639m

Bronchoalveolar lavage

Airway inflammation was assessed by differential enumeration of inflammatory cells in bronchoalveolar lavage fluid (BALF) as previously described [16]. Briefly, mice were anesthetized, after which the trachea was carefully exposed. A 20 G intravenous catheter was delicately inserted. 1 mL of Sterile PBS was gently infused into the lungs, followed by a series of gentle aspirations to retrieve the fluid. Transfer the fluid into a 15 mL tube placed on ice. Repeat these steps three times. After centrifugation at 1,000 g for 3 min, the pellets were resuspended in 1 mL PBS. Total and differential cell counts were assessed using a hemocytometer and a Diff-Quick stain kit (Sysmex, Kobe, Japan).

Immunofluorescence staining

For α-SMA visualization and quantification, MRC5 cells were treated as indicated and fixed in a 4% paraformaldehyde. Then, they were permeabilized using 0.5% PBS-Triton X-100 for 10 min and blocked with 5% goat serum for 1 h. Next, they were incubated with anti-α-SMA (1:200) antibody at room temperature for 4 h. Remove primary antibody solution and wash the cells three times with 1× PBS. Then the cells were stained by Alexa Fluor 488 secondary antibody for 1 h at room temperature. DAPI staining was used to determine the number of nuclei. The fluorescence was visualized by a SUNNY RX50 fluorescence microscope. An average score of the immunofluorescence intensity was normalized by the number of nuclei.

Luciferase reporter assay

The recombinant vector containing either wild-type (WT) or mutated (MT) 3'-UTR of FBXL16 was transfected into HEK293T cells or primary fibroblasts using Lipofectamine 3000. miRNA agomirs were subsequently transfected into cells depends upon the performance of experiments. The luciferase activity was measured 24 h after transfection.

Statistical analysis

Data is presented as mean ± SD. Statistical analyses were performed using GraphPad Prism 7.0 (GraphPad Software, La Jolla California USA). Differences between the groups were analyzed using Student's t-test or one-way ANOVA followed by Dunnett's multiple comparisons test. $p < 0.05$ was considered as significance.

Results

Mir-1307-5p is up-regulated in COPD patients

Firstly, we performed real-time PCR assay to confirm the expression of miR-1307-5p in the blood and lung samples from COPD patients. As expected, compared to normal counterparts, miR-1307-5p is increased in both kinds of samples derived from COPD patients (Fig. 1A and B). In addition, miR-1307-5p was up-regulated to a more pronounced extent in lung tissues than in blood, indicating that miR-1307-5p may be produced mainly by lung tissues in COPD. To further identify the major cell types in which miR-1307-5p was expressed, we isolated primary lung epithelial cells and fibroblasts from lung samples and determined miR-1307-5p expression by real-time PCR. The results showed that miR-1307-5p expression was considerably higher in lung fibroblasts from COPD patients, while in lung epithelial cells, the expression of miR-1307-5p increased somewhat but not significantly between COPD patients and normal participants (Fig. 1C and D). These results implicated that lung fibroblasts upregulated the expression of miR-1307-5p under COPD condition.

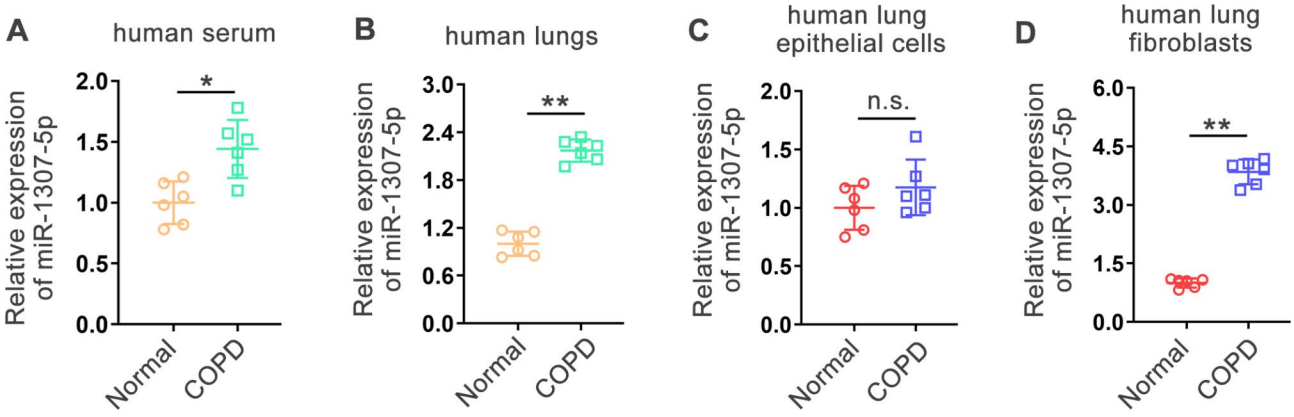

Fig. 1 MiR-1307-5p is increased in COPD. The abundance of miR-1307-5p in blood samples **(A)** or lung tissues **(B)** from COPD patients and normal counterparts ($n = 6$ per group). **(C-D)** The expression of miR-1307-5p in isolated primary human lung epithelial cells and fibroblasts. Data are presented as means ± SD. ns, no significance. *$p < 0.05$; **$p < 0.01$

Overexpression of mir-1307-5p exacerbates chronic smoking induced experimental COPD in mice

To further investigate the role of miR-1307-5p in COPD pathogenesis, we created an experimental COPD mouse model through chronic smoking exposure. As illustrated in Fig. 2A, overexpression of miR-1307-5p alone did not affect body weight gain in normally ventilated C57BL/6 mice, but it reduced body weight gain in mice exposed to chronic smoking. Additionally, ectopic expression of miR-1307-5p increased the number of inflammatory cells in alveolar lavage fluid, including total leukocytes, macrophages, and neutrophils (Fig. 2B). Histopathological analysis showed that overexpression of miR-1307-5p significantly exacerbated lung parenchymal tissue destruction induced by cigarette smoking (Fig. 2C and D). Furthermore, ectopic expression of miR-1307-5p elevated the levels of inflammatory cytokines (TNF-α and IL-6) and chemokines (CXCL1) in lung tissues (Fig. 2E, F and S1). In terms of lung function, miR-1307-5p overexpression markedly worsened pulmonary dysfunction caused by cigarette smoking (Fig. 2G and H). These findings suggest that miR-1307-5p is not only a biomarker in the blood of COPD patients but also plays a crucial role in COPD pathology.

Mir-1307-5p promotes lung fibroblasts transdifferentiation

The transdifferentiation of lung fibroblasts was crucial for COPD pathogenesis [19, 20]. TGF-β, a potent activator for fibroblast activation, was upregulated in COPD patients and CS-induced COPD mice compared with normal controls (Fig. S2). To explore the role of miR-1307-5p in lung fibroblasts, we treated human fetal lung fibroblasts MRC-5 with TGF-β. As shown in Fig. 3A, miR-1307-5p was dramatically increased after TGF-β treatment. Ectopic expression of miR-1307-5p in MRC-5 by agomir promoted cell transdifferentiation indicated by the markers of myofibroblast activation and ECM production, including α-SMA, calponin, collagen I, and fibronectin. Although overexpression of miR-1307-5p did not obviously activate fibroblasts in the absence of TGF-β stimulation, it markedly enhanced TGF-β induced fibroblasts transdifferentiation (Fig. 3B and C). Conversely, inhibition of intracellular miR-1307-5p using antagomir significantly suppressed myofibroblast differentiation induced by TGF-β (Fig. 3D).

Mir-1307-5p directly targets FBXL16 in COPD derived fibroblasts

MiRNAs function primarily by base pairing with the 3'-untranslated region (3'-UTR) of target mRNAs to negatively impact their protein output [21]. We performed in silico screen to find potential targets for miR-1307-5p in the regulation of fibroblast activation in TargetScan [22] and miRDB [23] database. We chose the top-ranked potential mRNAs and conducted further screening based on their significance to the processes associated with fibroblast differentiation using information from current research literature. The results showed that the seed region of miR-1307-5p matched the 3'-UTR of FBXL16 mRNA at two different locations (Fig. 4A). Overexpression of miR-1307-5p agomir in MRC-5 significantly repressed FBXL16 mRNA expression (Fig. 4B). To explore whether miR-1307-5p directly regulates FBXL16 expression, we constructed luciferase-expressing plasmids with either the wild-type (WT) or mutant (MT) 3'-UTR fragment of FBXL16 mRNA (Fig. 4C). As shown in Fig. 4D, miR-1307-5p agomir effectively suppressed luciferase expression with WT 3'-UTR, while having no effect with MT 3'-UTR, indicating that the regulation of miR-1307-5p on FBXL16 expression was dependent on the seed region sequence. We also introduced the luciferase plasmids into primary lung fibroblasts derived from normal subjects or COPD patients to test the influence of endogenous miR-1307-5p on FBXL16

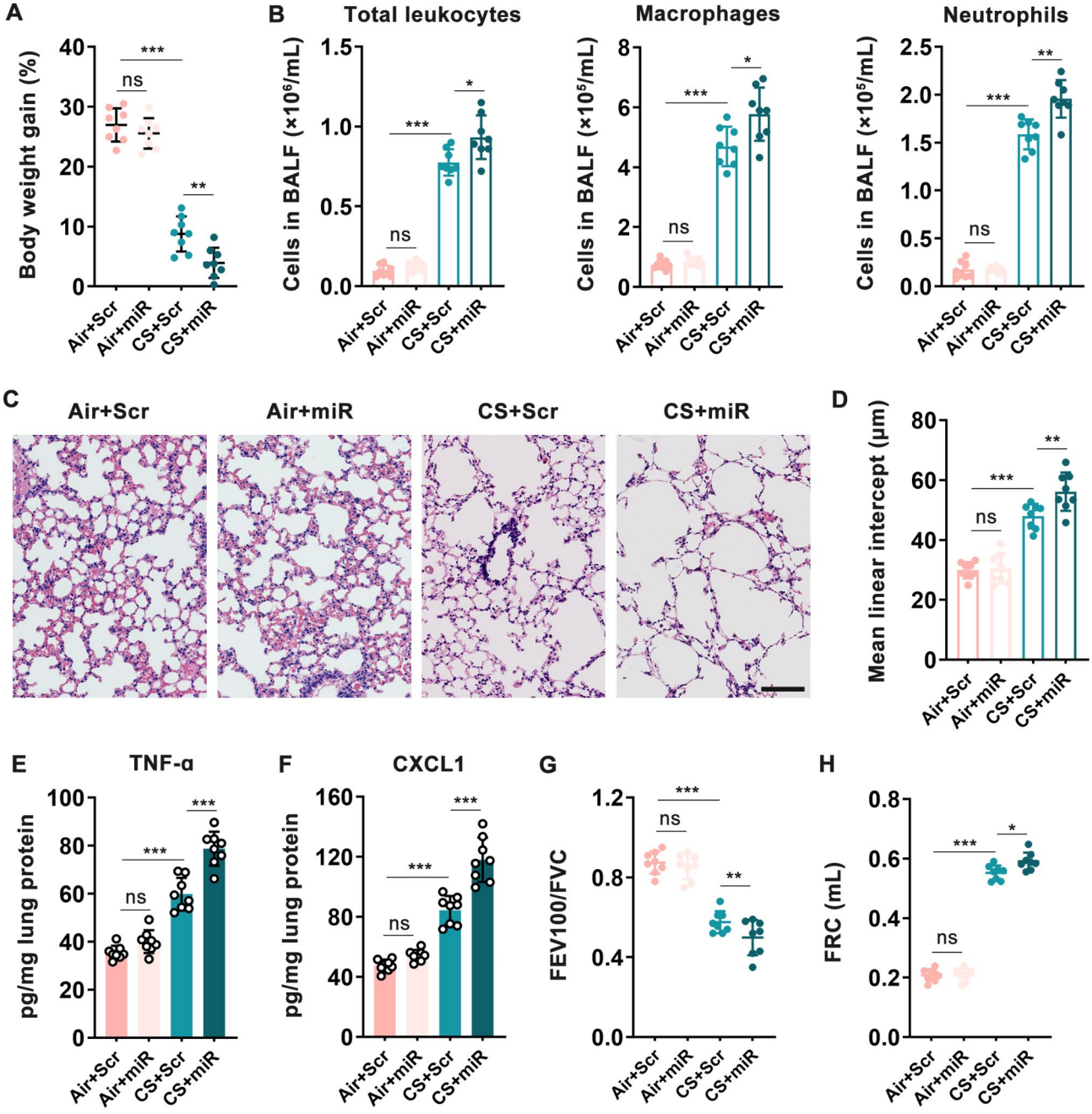

Fig. 2 Ectopic expression of miR-1307-5p exacerbates chronic smoking induced experimental COPD in mice. C57BL/6 mice were normally ventilated (Air) or exposed to chronic smoking (CS) for 16 weeks to induce experimental COPD. MiR-1307-5p agomir or scrambled (Scr) agomir were treated intranasally weekly. **(A)** The percentage of body weight gain. **(B)** The change of cells (total leukocytes, macrophages and neutrophils) in BALF. **(C)** Histological examination of lung tissues stained by hematoxylin-eosin staining. Scale bar, 100 μm. **(D)** The mean linear intercept of lung tissues calculated based on (C). **(E, F)** TNF-α and CXCL1 proteins in whole-lung homogenates were measured by ELISA. Pulmonary function, including FEV100/FVC **(G)** and functional residual capacity (FRC) **(H)** were calculated ($n = 8$ mice per group). Data are presented as means ± SD. ns, no significance. *$p < 0.05$; **$p < 0.01$; ***$p < 0.001$

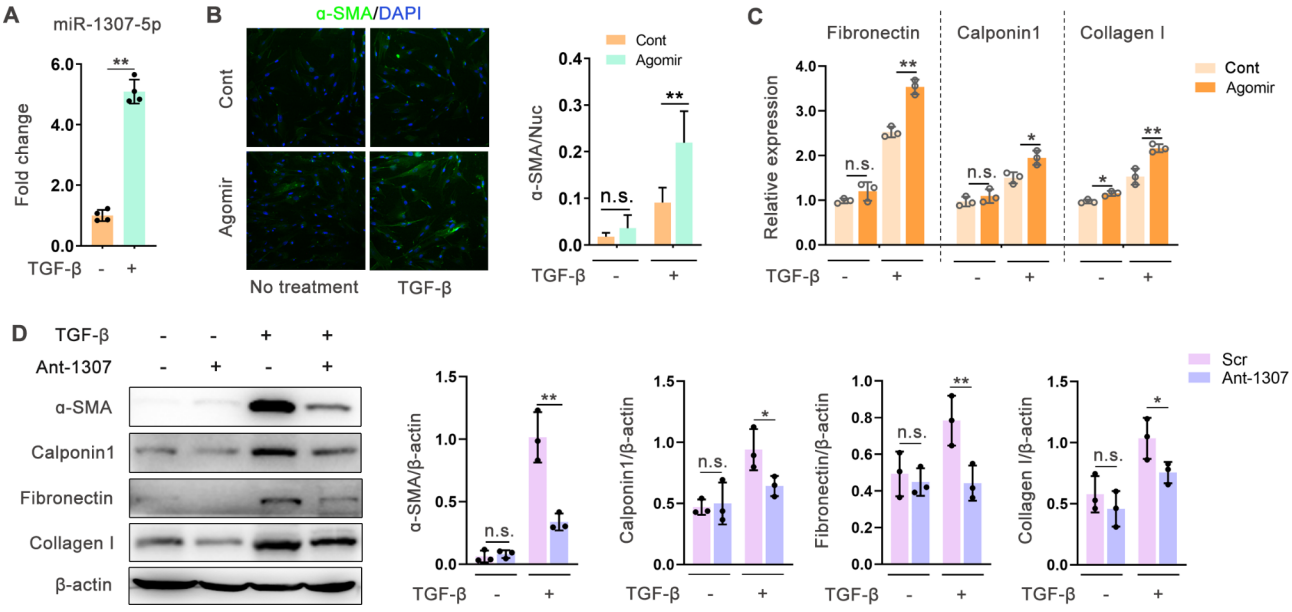

Fig. 3 MiR-1307-5p promotes transdifferentiation of lung fibroblasts. **(A)** Human lung fibroblasts MRC-5 were treated with TGF-β for 72 h. The expression of miR-1307-5p was measured by real-time PCR ($n=4$). **(B-C)** MRC-5 were transfected with 50 nM control oligos (Cont) or miR-1307-5p agomir (Agomir). Three days after transfection, cells were collected. **(B)** Representative immunofluorescence staining and quantification of α-SMA in MRC-5 fibroblasts cultured with 2 ng/mL TGF-β for 72 h. Eight images were captured per treatment and normalized to the number of nuclei for quantification. **(C)** The expression of markers for lung fibroblast (MRC-5) transdifferentiation were determined by real-time PCR ($n=3$). **(D)** MRC-5 were transfected with control oligos (Scr) or miR-1307-5p antagomir (Ant-1307) and were cultured with or without TGF-β. The markers of fibroblast differentiation were determined by western blotting ($n=3$). The intensity of bands was calculated and normalized by β-actin expression. Data are presented as means ± SD. n.s., not significant. *$p<0.05$; **$p<0.01$

expression. As shown in Fig. 4E, luciferase expression with WT 3'-UTR was significantly repressed only in COPD fibroblasts, comparing to normal fibroblasts, indicating higher endogenous miR-1307-5p under COPD condition. Although luciferase expression was reduced with MT 3'-UTR in COPD fibroblasts, the difference was not significant, implying that miR-1307-5p may have a major role in the control of FBXL16 expression in COPD fibroblasts.

FBXL16 inhibits TGF-β induced transdifferentiation in lung fibroblasts

The link between FBXL16 and myofibroblast activation has yet to be established. We found that FBXL16 expression was decreased in TGF-β induced MRC-5 (Fig. 5A). Knockdown of FBXL16 by siRNA prominently increased the expression of markers with myofibroblast differentiation after TGF-β administration (Fig. 5B). Similar to the effect of miR-1307-5p overexpression, knockdown of FBXL16 alone was not sufficient to induce MRC-5 transdifferentiation in the absence of TGF-β treatment (Fig. 5B). FBXL16 ectopic expression, on the other hand, significantly suppressed TGF-β-induced activation of MRC-5, as shown by α-SMA immunofluorescence staining (Fig. 5C) and the protein expression of myofibroblast activation biomarkers (Fig. 5D).

Replenishment of FBXL16 alleviates CS-induced experimental COPD in mice

To further explore the role of FBXL16 in COPD progression in vivo, we overexpressed FBXL16 in murine lungs by intranasally administering control or FBXL16-expressing AAV6 to mice during chronic smoking exposure. As depicted in Fig. 6A, chronic smoking (CS) significantly decreased FBXL16 expression, whereas AAV6-FBXL16 administration significantly increased FBXL16 levels under both normally ventilated and chronic smoking conditions. Overexpression of FBXL16 did not affect body weight gain in normally ventilated C57BL/6 mice but increased body weight gain in mice exposed to chronic smoking (Fig. 6B). Additionally, ectopic expression of FBXL16 reduced the number of inflammatory cells in alveolar lavage fluid, including total leukocytes, macrophages, and neutrophils in CS challenged mice (Fig. 6C and S3). Histopathological analysis showed that overexpression of FBXL16 significantly ameliorated lung parenchymal tissue destruction induced by cigarette smoking (Fig. 6D and E). Furthermore, ectopic expression of FBXL16 reduced the levels of inflammatory cytokines (TNF-α) and chemokines (CXCL1) in lung tissues (Fig. 6F and G). Moreover, FBXL16 overexpression markedly improved pulmonary dysfunction caused by cigarette smoking (Fig. 6H and I). These in vivo findings, along with previous in vitro investigations, underscore

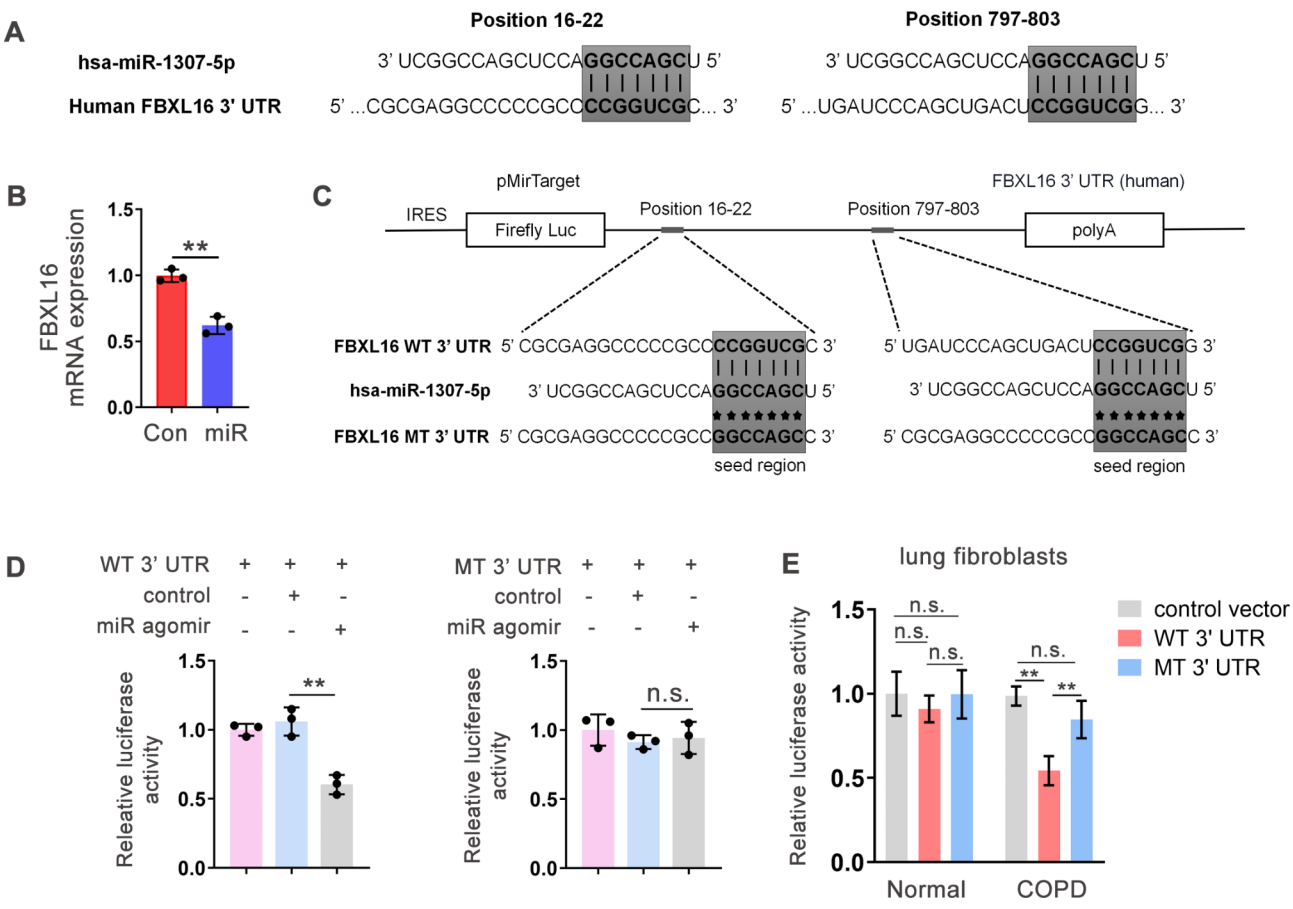

Fig. 4 miR-1307-5p directly targets FBXL16 mRNA. **(A)** The seed region of miR-1307-5p predicted to target the 3′UTR of FBXL16 in human. **(B)** MRC-5 cells were transfected with control or miR-1307-5p agomir (miR). The mRNA level of FBXL16 was measured by real-time PCR 24 h after transfection ($n=3$). **(C)** Depiction of luciferase reporter construct for wild-type (WT) and mutated (MT) 3′-UTR of the FBXL16 seed region. **(D)** 293T cells were transfected with 50 ng of either pMirTarget vector carrying WT or mutated 3′UTR of FBXL16 with or without 50 nM miR-1307-5p agomir. **(E)** The lung fibroblasts derived from normal or COPD lung tissues were transfected with luciferase reporter construct carrying either WT or MT 3′UTR of FBXL16 ($n=3$). Data are presented as means ± SD. n.s., not significant. $^{**}p<0.01$

the critical role of FBXL16 in COPD, particularly in pulmonary fibroblast activation.

Mir-1307-5p enhances lung myofibroblast activation through inhibition of FBXL16

To further determine whether miR-1307-5p enhances lung myofibroblast activation via FBXL16, we examined FBXL16 expression in TGF-β treated MRC-5 cells with and without miR-1307-5p suppression. The result showed that inhibition of miR-1307-5p restored TGF-β induced reduction of FBXL16 (Fig. 7A). Re-suppression of FBXL16 by siRNA largely abolished the inhibitory effect of miR-1307-5p antagomir on myofibroblast activation in TGF-β treated MRC-5, indicated by α-SMA immunofluorescence staining (Fig. 7B). Conversely, supplementation of FBXL16 in MRC-5 obviously counteracted miR-1307-5p agomir-induced cell transdifferentiation (Fig. 7C).

MiR-1307-5p enhances fibroblast transdifferentiation through inhibiting FBXL16/HIF1α axis

HIF1α promotes TGF-β induced expression of profibrotic genes in activated alveolar macrophages in pulmonary fibrosis [24]. Hypoxia induced HIF1α stimulation promotes epithelial-to-mesenchymal transition and fibrogenesis in patients with chronic kidney disease [25]. Additionally, HIF1α has been demonstrated to play a crucial role in the pathological process of COPD [26, 27]. We examined HIF1α expression in primary human lung fibroblasts derived from COPD patients and normal counterparts. The result showed that the expression of HIF1α mRNA was obviously increased in COPD (Fig. 8A). Overexpression of HIF1α further enhanced TGF-β induced pulmonery fibroblast activation (Fig. 8B and C). In contrast, the expression of FBXL16 mRNA was obviously decreased in COPD patients (Fig. 8A). Furthermore, we observed that HIF1α and FBXL16 appeared to be up-regulated and down-regulated, respectively, in the lungs of CS-induced COPD mice (Fig. 8D). It is reported

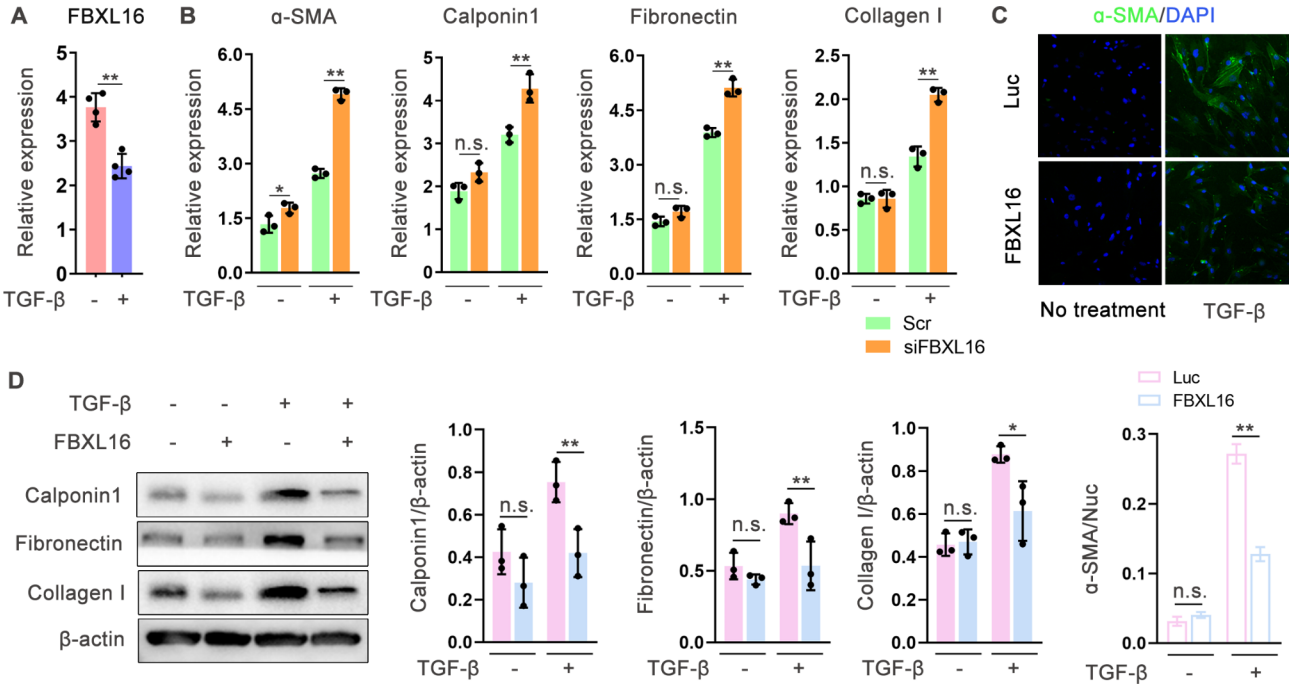

Fig. 5 FBXL16 inhibits transdifferentiation of lung fibroblasts. MRC-5 were treated with 2 ng/mL TGF-β for 72 h. **(A)** The expression of FBXL16 was measured by real-time PCR ($n=4$). **(B)** The cells were transfected with siRNA targeting FBXL16 (siFBXL16) or control siRNA (Scr). The markers of lung fibroblast activation were determined by real-time PCR ($n=3$). **(C-D)** MRC-5 cells were transfected with control (Luc) or FBXL16 expressing plasmids. Three days after transfection, the cells were collected. **(C)** Upper, representative immunofluorescence staining of α-SMA was shown; lower, the quantitatived value of α-SMA staining intensity in MRC-5 was normalized to the number of nuclei. **(D)** The markers of lung fibroblast activation were determined by real-time PCR ($n=3$). The values were normalized by β-actin expression. Data are presented as means ± SD. n.s., not significant. *$p<0.05$; **$p<0.01$

that FBXL16 suppresses breast cancer progression via regulation of HIF1α stability [28]. In COPD mice, overexpression of FBXL16 using AAV6 effectively reduced the abundance of HIF1α protein (Fig. 8D). Additionally, ectopic expression of FBXL16 in vitro can significantly inhibit the promotion of TGF-β-induced fibroblast transdifferentiation by HIF1α overexpression, as indicated by the decreased protein expression of myofibroblast activation biomarkers (Fig. 8E). Furthermore, we validated the regulatory role of miR-1307-5p on HIF1α in MRC-5 cells, discovering that overexpression of miR-1307-5p further increased TGF-β-induced HIF1α protein accumulation (Fig. 8F). These findings suggest that miR-1307-5p regulates fibroblast transdifferentiation through the FBXL16/HIF1α axis. To further confirm miR-1307-5p regulates FBXL16/HIF1α axis in vivo, we examined the protein abundance of HIF1α and FBXL16 in the lungs of mice treated intranasally miR-1307-5p or scrambled agomir. The result showed that overexpression of miR-1307-5p repressed FBXL16 and enhanced HIF1α accumulation in both normally ventilated and smoke exposed mice. The manifestation of this regulatory effect is even more pronounced under the pathological conditions of COPD induced by smoke exposure (Fig. 8G).

Discussion

In this study, we investigated the role of miR-1307-5p in the pathogenic progress of COPD. We searched for and validated the targets of miR-1307-5p in the regulation of lung fibroblast activation. Based on an in vitro model, we found that the up-regulation of miR-1307-5p that promoted the transdifferentiation of lung fibroblasts mainly through the inhibition of FBXL16 and increase of HIF1α accumulation.

FBXL16 is a poorly studied F-box protein which consists of an N-terminal Proline-rich domain, an F-box motif and a C-terminal domain of Leucine-rich repeats. FBXL16 was first identified as a transcriptional target of E2F1 [29] and was then showed as a binding partner of PP2A (Protein Phosphatase 2 A) and as a regulator of its phosphatase activity [30]. In mice, homozygous knockout of the FBXL16 gene causes perinatal death, while FBXL16 depletion increased development of mouse embryonic stem cells along the cardiomyocyte lineage, implying that FBXL16 plays important physiological roles [30, 31]. However, existing reports on the intracellular function of FBXL16 are inconsistent. The expression of FBXL16 was downregulated in triple-negative breast cancer (TNBC). FBXL16 directly binds to HIF1α and induces its ubiquitination and degradation, regardless of the tumor microenvironment, reducing the impact of HIF1α-mediated

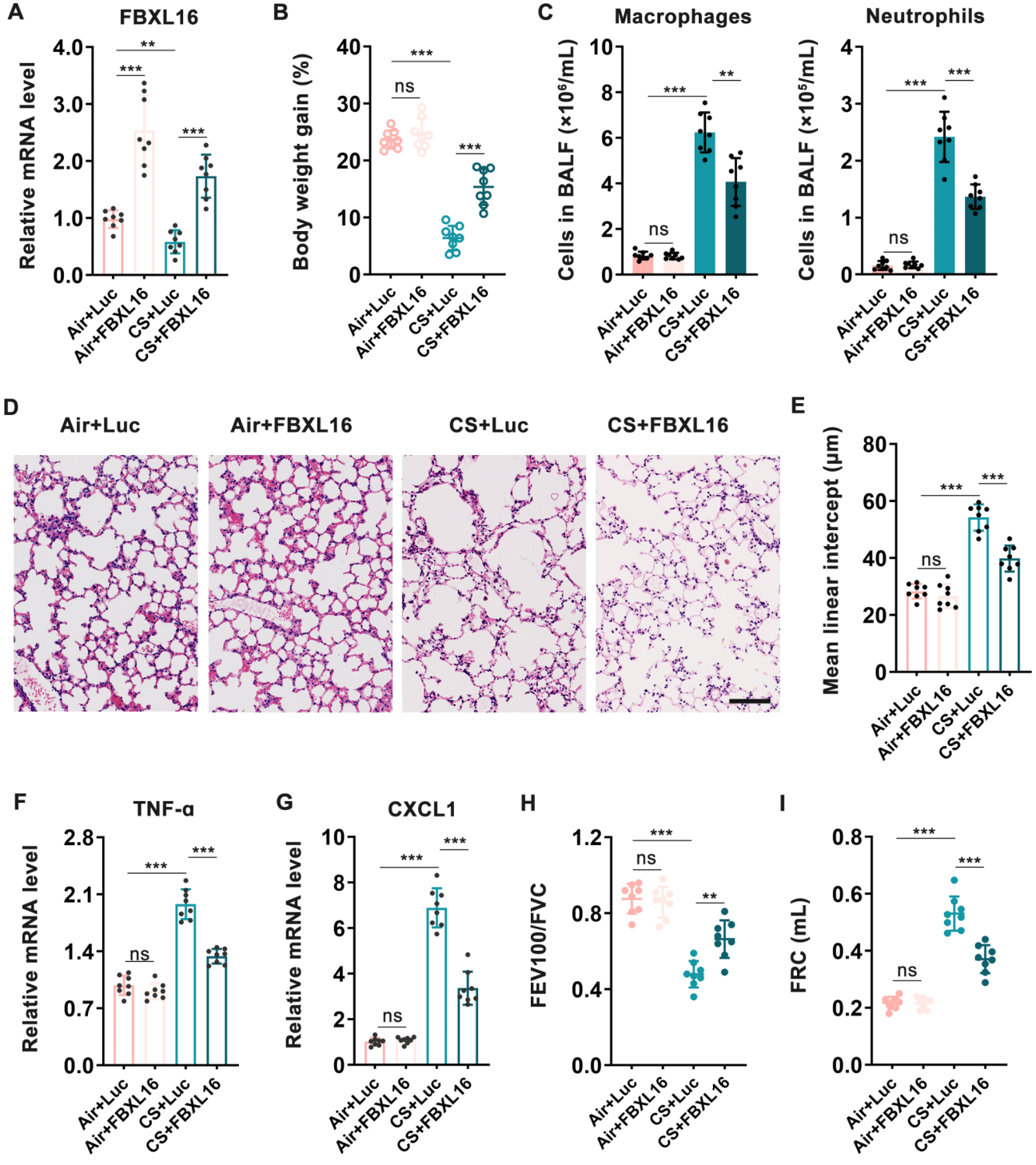

Fig. 6 Replenishment of FBXL16 alleviates CS-induced experimental COPD in mice. C57BL/6 mice were normally ventilated (Air) or exposed to chronic smoking (CS) for 16 weeks to induce experimental COPD. Mice were intranasally administered with control (Luc, AAV6-expressing luciferase reporter) or FBXL16 expressing AAV6 twice. **(A)** The relative mRNA level of FBXL16 in mice after AAV6-FBXL16 treatment. **(B)** The percentage of body weight gain of mice after CS challenge with or without AAV6-FBXL16 treatment. **(C)** Macrophages and neutrophils were enumerated in bronchoalveolar lavage fluid (BALF) ($n=8$ mice per group). **(D)** Histological examination of lung tissues stained by hematoxylin-eosin staining. Scale bar, 100 μm. **(E)** The mean linear intercept of lung tissues calculated based on (D). The change of TNF-α **(F)** and CXCL1 **(G)** protein in whole-lung homogenates. **(H-I)** Pulmonary function, including FEV100/FVC and FRC were determined ($n=8$ mice per group). Data are presented as means ± SD. ns, no significance. *$p<0.05$; **$p<0.01$; ***$p<0.001$

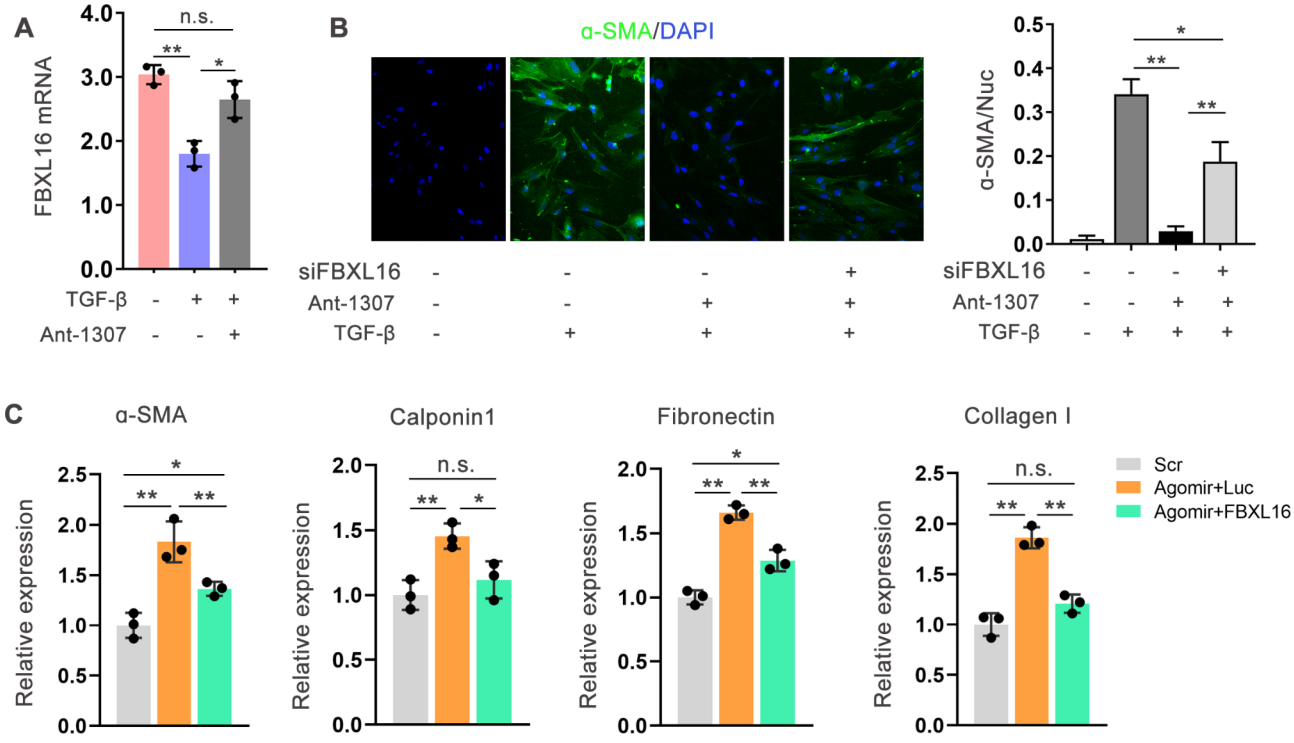

Fig. 7 miR-1307-5p enhances lung fibroblast differentiation through inhibition of FBXL16. **(A)** MRC-5 were treated as indicated. The expression of FBXL16 was measured by real-time PCR ($n=3$). **(B)** MRC-5 cells were transfected with siRNA targeting FBXL16 (siFBXL16) and/or miR-1307-5p antagomir (Ant-1307) for 72 h after TGF-β treatment. Representative images of immunofluorescence staining and quantification of α-SMA expression were shown. **(C)** MRC-5 cells were transfected with miR-1307-5p agomir (Agomir) and control (Luc) or FBXL16 expressing plasmids for 72 h after TGF-β treatment. The markers of lung fibroblast differentiation were determined by real-time PCR ($n=3$). The values were normalized by β-actin expression. Data are presented as means ± SD. n.s., not significant. $^{*}p<0.05$; $^{**}p<0.01$

EMT and angiogenesis potential of breast cancer. Ectopic expression of FBXL16 significantly inhibited lung metastasis of TNBC [28]. However, as an E3 ligase, FBXL16 antagonizes FBW7-mediated polyubiquitination and degradation of c-myc and promotes cancer cell growth and migration in lung cancer cells [31].

To date, there is a lack of available literature regarding the involvement of FBXL16 in other pulmonary disorders. By comparative analysis of gene expression profiling data from lung tissues of healthy individuals and COVID-19-infected individuals [32], we found that COVID-19 infection significantly reduces the expression of FBXL16 in lung tissues (Fig. S4). It is known that COVID-19 infection causes pulmonary fibrosis, and it is worth investigating whether FBXL16 is involved. The current investigation revealed that FBXL16 effectively suppressed TGF-β induced transdifferentiation of lung fibroblasts to myofibroblasts. Nevertheless, the mere manipulation of miR-1305-5p expression levels through knockdown or overexpression in MRC-5 lung fibroblasts did not yield noteworthy cellular transdifferentiation outcomes. Inhibition of FBXL16 by siRNA or overexpression of miR-1305-5p appeared to either sensitize the cellular response to TGF-β or to establish a preactivated state in cells to TGF-β induction. The promotion of lung fibroblast activation by FBXL16 inhibition was dependent on the TGF-β treatment, indicating a potential association between FBXL16 and the TGF-β signaling pathway. The details of particular relationship between FBXL16 and TGF-β are warranted in future investigations.

COPD is characterized by airflow limitations that are not fully reversible, and it is closely associated with hypoxia, a condition where the body's tissues receive insufficient oxygen. Hypoxia is a key factor in the development and progression of COPD, as it can lead to the overexpression of HIF-1α, the transcription factor that plays a crucial role in the body's response to low oxygen levels. The relationship between COPD and HIF-1α is complex and bidirectional. While hypoxia-induced HIF-1α contributes to COPD pathogenesis, COPD itself can also create a hypoxic environment that further stimulates HIF-1α expression, creating a vicious cycle that can lead to more severe disease manifestations. HIF-1α is involved in the regulation of various genes that are associated with angiogenesis, inflammation, and cell survival. In the context of COPD, HIF-1α has been found to be overexpressed, which can contribute to the inflammatory response and disease progression. The overexpression of

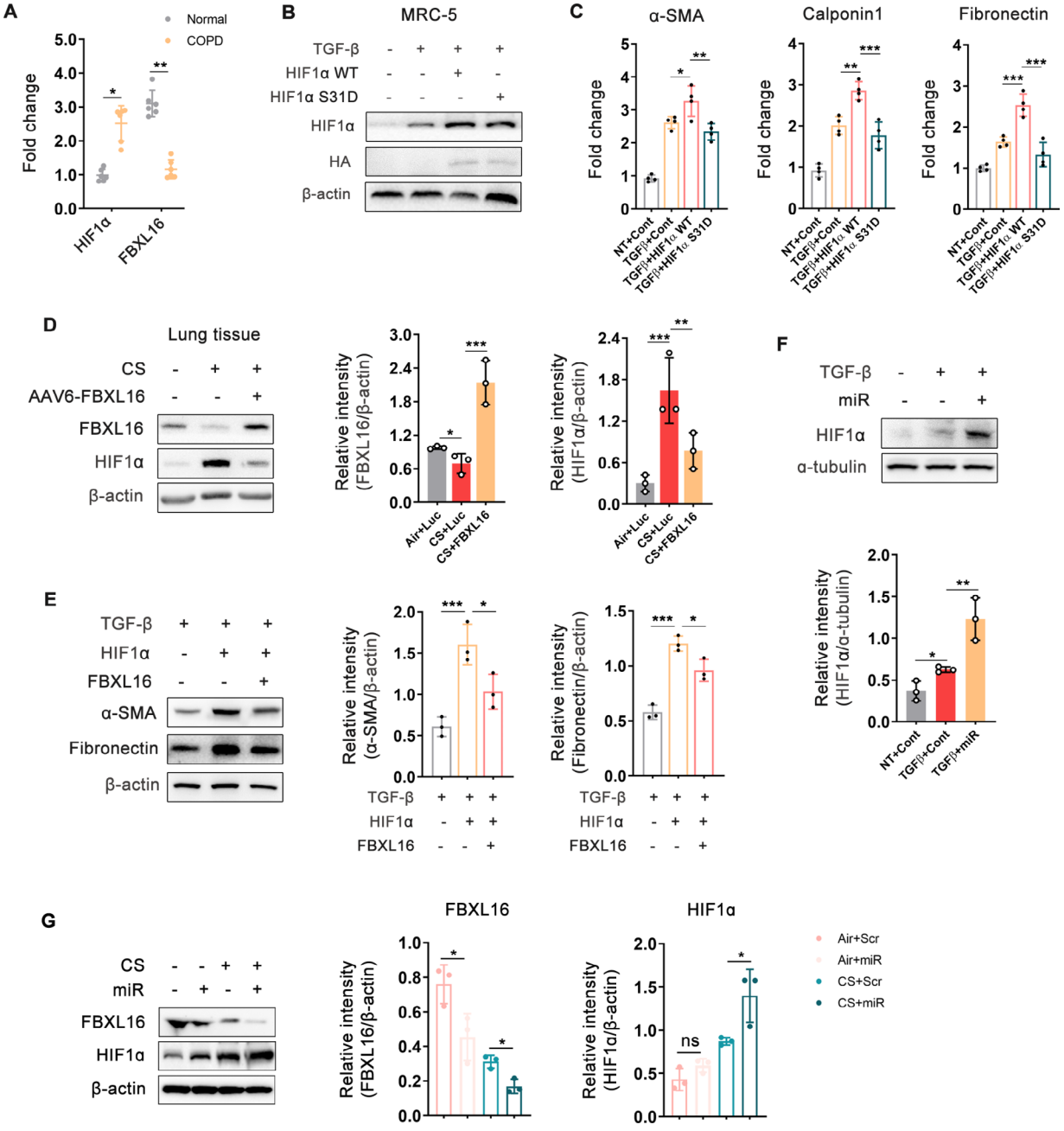

Fig. 8 HIF1α mediates FBXL16 regulated fibroblast activation. **(A)** The mRNA expression of HIF1α and FBXL16 in isolated primary human lung fibroblasts derived from COPD patients and normal counterparts ($n=6$ per group). **(B)** MRC-5 were transfected with wild type and point mutated (S31D) HIF1α and treated as indicated. The expression of HIF1α was determined by western blotting. HA-tag was detected to confirm ectopic expression of HIF1α. **(C)** The markers of fibroblast transdifferentiation from (B) were determined by real-time PCR ($n=3$). The values were normalized by β-actin expression. **(D)** C57BL/6 mice were normally ventilated (Air) or exposed to chronic smoking (CS) for 16 weeks to induce experimental COPD. Mice were intranasally administered with control or FBXL16 expressing AAV6 twice. The protein abundance of HIF1α and FBXL16 in the lungs of mice were measured. Left, the representative result was shown; right, the intensity of bands was calculated by ImageJ and normalized by β-actin expression ($n=3$). **(E)** MRC-5 cells were transfected with HIF1α and/or FBXL16 expressing plasmid and treated by TGF-β as indicated. The markers of lung fibroblast activation (α-SMA and fibronetion) were determined. Left, the representative result was shown; right, the intensity of bands was calculated by ImageJ and normalized by β-actin expression ($n=3$). **(F)** MRC-5 cells were transfected with control or miR-1307-5p agomir (miR) and treated by TGF-β as indicated. The protein abundance of HIF1α was measured. Left, the representative result was shown; right, the intensity of bands was calculated by ImageJ and normalized by α-tubulin expression ($n=3$). **(G)** C57BL/6 mice were normally ventilated (Air) or exposed to chronic smoking (CS) for 16 weeks to induce experimental COPD. MiR-1307-5p agomir (miR) or scrambled (Scr) agomir were treated intranasally weekly. The protein abundance of HIF1α and FBXL16 in the lungs of mice were measured by western blotting. Left, the representative result was shown; right, the intensity of bands was calculated by ImageJ and normalized by β-actin expression ($n=3$). Data are presented as means ± SD. n.s., not significant. $^{*}p<0.05$; $^{**}p<0.01$; $^{***}p<0.001$

HIF-1α can lead to the activation of the EGFR/PI3K/AKT pathway, which in turn can increase the levels of inflammatory factors, thus exacerbating COPD pathology [26]. Moreover, HIF-1α is implicated in the hypercoagulable state observed in COPD, which is a prothrombotic condition that can contribute to the development of pulmonary hypertension and right-sided heart failure, both of which are complications of COPD. The HIF-1α-EPO/EDN-1/VEGF pathway is suggested to play an important role in this hypercoagulable state [33], and targeting this pathway could potentially improve outcomes in COPD.

On the basis of our previous study, we further explored the reasons for the increase of miR-1307-5p in the blood of COPD patients and its regulatory role on the pathological progression of COPD. There are several limitations in our study. We did not conduct an in-depth examination of the mechanism by which miR-1307-5p was up-regulated in COPD, which may pose some challenges to using miR-1307-5p as an intervention target for COPD therapy. We will perform more in-depth research depending on the application needs in the follow-up study.

In the clinical samples, we found that the expression of miR-1307-5p in alveolar epithelial cells and fibroblasts in COPD patients compared to the healthy counterparts is differential. Although in this study we focused on fibroblasts, whether miR-1307-5p also plays a role in EMT in epithelial cells is also a question that deserves further exploration. Indeed, EMT transformation of alveolar epithelial cells under the influence of chronic irritants such as smoke is also an important molecular pathological cause of COPD development and progression. We did not differentiate epithelial cells from airway and lung parenchymal tissues according to the sampling site, and we did not use single-cell sequencing to subdivide different epithelial cell subpopulations, which may mask the differences in the expression of MiR-1307-5p among different populations of epithelial cells. Of course, there have been many studies exploring the molecular mechanisms of EMT transformation in epithelial cells during COPD, and even if miR-1307-5p does play a role through the FBXL16/HIF1α axis, which is one of the mechanisms, the specific pathway selection by cells in this case, and and the nuanced outcomes that arise from this process remain intriguing areas for future research.

In general, our investigation enhances the comprehension of the involvement of miRNAs in the progression of COPD. Our data suggest that miR-1307-5p plays a crucial role in COPD etiology and may be a potential target for COPD treatment.

Supplementary Information

The online version contains supplementary material available at https://doi.org/10.1186/s12931-024-03007-6.

Supplementary Material 1

Supplementary Material 2

Supplementary Material 3

Supplementary Material 4

Supplementary Material 5

Supplementary Material 6

Supplementary Material 7

Author contributions

Participated in research design: F. Zhang, C. S. Chen, F. Lu, L. P. Yao Conducted experiments: L. P. Yao, Z. K. Wang, X. Q. Jiang, D. D. Gao, B. E. Jiang, S. J. Chen, Z. D. Hua Performed data analysis: Q. Zheng, L. F. Xu, M. X. Qian, S. M. Zhu, F. ZhangWrote or contributed to the writing of the manuscript: F. Zhang, L. F. Xu, C. S. Chen, F. Lu.

Funding

This work was supported by Quzhou technology projects [2023K109, 2022K46], Natural Science Foundation of China [82370085, 82170017, 81502304], Natural Science Foundation of Zhejiang Province [LGF22G010009], Medical and Health Technology Projects of Zhejiang Province [2017KY696, 2019PY089], Chinese Medicine Science Foundation of Zhejiang Province [2021ZB328].

Data availability

No datasets were generated or analysed during the current study.

Declarations

Ethical approval

All studies have been approved by the Institutional Review Board at the Quzhou Affiliated Hospital of Wenzhou Medical University. Each patient signed an informed consent form for sample collection.

Consent for publication

Not Applicable.

Conflict of interest

The authors declare that they have no known competing financial interests or personal relationships that could have appeared to influence the work reported in this paper.

Received: 19 July 2024 / Accepted: 8 October 2024
Published online: 17 October 2024

References

1. Christenson SA, et al. Chronic obstructive pulmonary disease. Lancet. 2022;399(10342):2227–42.
2. Celli BR, Wedzicha JA. Update on clinical aspects of Chronic Obstructive Pulmonary Disease. N Engl J Med. 2019;381(13):1257–66.
3. Jones RL, et al. Airway remodelling in COPD: it's not asthma! Respirology. 2016;21(8):1347–56.
4. Karakioulaki M, Papakonstantinou E, Stolz D. Extracellular matrix remodelling in COPD. Eur Respir Rev, 2020. 29(158).
5. Eapen MS et al. Increased myofibroblasts in the small airways, and relationship to remodelling and functional changes in smokers and COPD patients: potential role of epithelial-mesenchymal transition. ERJ Open Res, 2021. 7(2).
6. White ES. Lung extracellular matrix and fibroblast function. Ann Am Thorac Soc. 2015;12(Suppl 1):S30–3.
7. Burgess JK, et al. The extracellular matrix - the under-recognized element in lung disease? J Pathol. 2016;240(4):397–409.
8. Hallgren O, et al. Enhanced ROCK1 dependent contractility in fibroblast from chronic obstructive pulmonary disease patients. J Transl Med. 2012;10:171.

9. Saito A, Horie M, Nagase T. TGF-beta signaling in Lung Health and Disease. Int J Mol Sci, 2018. 19(8).
10. Karvonen HM, et al. Myofibroblast expression in airways and alveoli is affected by smoking and COPD. Respir Res. 2013;14(1):84.
11. Togo S, et al. Lung fibroblast repair functions in patients with chronic obstructive pulmonary disease are altered by multiple mechanisms. Am J Respir Crit Care Med. 2008;178(3):248–60.
12. Ha M, Kim VN. Regulation of microRNA biogenesis. Nat Rev Mol Cell Biol. 2014;15(8):509–24.
13. Gebert LFR, MacRae IJ. Regulation of microRNA function in animals. Nat Rev Mol Cell Biol. 2019;20(1):21–37.
14. Hobbs BD, Tantisira KG. MicroRNAs in COPD: small molecules with big potential. Eur Respir J, 2019. 53(4).
15. Du X, et al. MiR-1307-5p targeting TRAF3 upregulates the MAPK/NF-kappaB pathway and promotes lung adenocarcinoma proliferation. Cancer Cell Int. 2020;20:502.
16. Lu F, et al. MicroRNA-377-3p exacerbates chronic obstructive pulmonary disease through suppressing ZFP36L1 expression and inducing lung fibroblast senescence. Respir Res. 2024;25(1):67.
17. Guan R et al. Bone morphogenetic protein 4 inhibits pulmonary fibrosis by modulating cellular senescence and mitophagy in lung fibroblasts. Eur Respir J, 2022. 60(6).
18. Sheng H, et al. YEATS2 regulates the activation of TAK1/NF-kappaB pathway and is critical for pancreatic ductal adenocarcinoma cell survival. Cell Biol Toxicol. 2023;39(3):1–16.
19. Woldhuis RR, et al. COPD-derived fibroblasts secrete higher levels of senescence-associated secretory phenotype proteins. Thorax. 2021;76(5):508–11.
20. Krimmer DI, et al. Matrix proteins from smoke-exposed fibroblasts are pro-proliferative. Am J Respir Cell Mol Biol. 2012;46(1):34–9.
21. Wilczynska A, Bushell M. The complexity of miRNA-mediated repression. Cell Death Differ. 2015;22(1):22–33.
22. Agarwal V et al. Predicting effective microRNA target sites in mammalian mRNAs. Elife, 2015. 4.
23. Chen Y, Wang X. miRDB: an online database for prediction of functional microRNA targets. Nucleic Acids Res. 2020;48(D1):D127–31.
24. Ueno M, et al. Hypoxia-inducible factor-1alpha mediates TGF-beta-induced PAI-1 production in alveolar macrophages in pulmonary fibrosis. Am J Physiol Lung Cell Mol Physiol. 2011;300(5):L740–52.
25. Higgins DF, et al. Hypoxia promotes fibrogenesis in vivo via HIF-1 stimulation of epithelial-to-mesenchymal transition. J Clin Invest. 2007;117(12):3810–20.
26. Zhang HX, et al. HIF-1alpha promotes inflammatory response of chronic obstructive pulmonary disease by activating EGFR/PI3K/AKT pathway. Eur Rev Med Pharmacol Sci. 2018;22(18):6077–84.
27. Fu X, Zhang F. Role of the HIF-1 signaling pathway in chronic obstructive pulmonary disease. Exp Ther Med. 2018;16(6):4553–61.
28. Kim YJ, et al. Suppression of breast cancer progression by FBXL16 via oxygen-independent regulation of HIF1alpha stability. Cell Rep. 2021;37(8):109996.
29. Sato K, et al. FBXL16 is a novel E2F1-regulated gene commonly upregulated in p16INK4A- and p14ARF-silenced HeLa cells. Int J Oncol. 2010;36(2):479–90.
30. Honarpour N, et al. F-box protein FBXL16 binds PP2A-B55alpha and regulates differentiation of embryonic stem cells along the FLK1 + lineage. Mol Cell Proteom. 2014;13(3):780–91.
31. Morel M, Shah KN, Long W. The F-box protein FBXL16 up-regulates the stability of C-MYC oncoprotein by antagonizing the activity of the F-box protein FBW7. J Biol Chem. 2020;295(23):7970–80.
32. Wang S, et al. A single-cell transcriptomic landscape of the lungs of patients with COVID-19. Nat Cell Biol. 2021;23(12):1314–28.
33. Deng R, et al. Role of HIF-1alpha in hypercoagulable state of COPD in rats. Arch Biochem Biophys. 2024;753:109903.

Publisher's note